

Abscisic Acid Acts as a Blocker of the Bitter Taste G Protein-Coupled Receptor T2R4

Sai P. Pydi,[†] Appalaraju Jaggupilli,[†] Ken M. Nelson,^{||} Suzanne R. Abrams,^{||} Rajinder P. Bhullar,[†] Michele C. Loewen,^{‡,§} and Prashen Chelikani^{*,†}

[†]Department of Oral Biology, University of Manitoba, Winnipeg, MB R3E 0W4, Canada

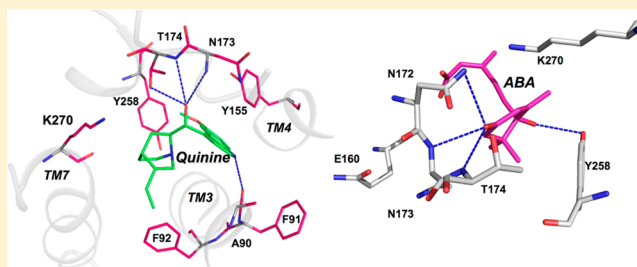
[‡]National Research Council of Canada, 110 Gymnasium Place, Saskatoon, SK S7N 0W9, Canada

[§]Department of Biochemistry, University of Saskatchewan, 105 Wiggins Road, Saskatoon, SK S7N 5N5, Canada

^{||}Department of Chemistry, University of Saskatchewan, 110 Science Place, Saskatoon, SK S7N 5C9, Canada

Supporting Information

ABSTRACT: Bitter taste receptors (T2Rs) belong to the G protein-coupled receptor superfamily. In humans, 25 T2Rs mediate bitter taste sensation. In addition to the oral cavity, T2Rs are expressed in many extraoral tissues, including the central nervous system, respiratory system, and reproductive system. To understand the mechanistic roles of the T2Rs in oral and extraoral tissues, novel blockers or antagonists are urgently needed. Recently, we elucidated the binding pocket of T2R4 for its agonist quinine, and an antagonist and inhibitory neurotransmitter, γ -aminobutyric acid. This structure–function information about T2R4 led us to screen the plant hormone abscisic acid (ABA), its precursor (xanthoxin), and catabolite phaseic acid for their ability to bind and activate or inhibit T2R4. Molecular docking studies followed by functional assays involving calcium imaging confirmed that ABA is an antagonist with an IC_{50} value of $34.4 \pm 1.1 \mu\text{M}$. However, ABA precursor xanthoxin acts as an agonist on T2R4. Interestingly, molecular model-guided site-directed mutagenesis suggests that the T2R4 residues involved in quinine binding are also predominantly involved in binding to the novel antagonist, ABA. The antagonist ability of ABA was tested using another T2R4 agonist, yohimbine. Our results suggest that ABA does not inhibit yohimbine-induced T2R4 activity. The discovery of natural bitter blockers has immense nutraceutical and physiological significance and will help in dissecting the T2R molecular pathways in various tissues.



Taste receptor cells present in taste buds on the tongue express a number of membrane proteins that mediate taste sensation. In humans, bitter taste is one of the five basic taste sensations and is mediated by 25 bitter taste receptors (T2Rs).^{1,2} Recent studies have shown that T2Rs are also expressed outside the tongue, including many extraoral tissues such as central nervous system, respiratory system, digestive system, and male reproductive system.^{3–7} This suggests that T2Rs possess as yet largely uncharacterized cellular and physiological functions in addition to taste sensing. Most of the T2Rs are activated by a wide variety of plant-derived bitter compounds, including amides, heterocyclic compounds, glycosides, alkaloids, terpenoids, phenols, and flavonoids.⁸ A few plant-derived compounds like, 6-methoxyflavanones and sesquiterpene lactones, are known to block T2R39 and T2R46, respectively.^{9,10} However, no literature about the effect of phytohormones on T2Rs activity is available.

Recently, we elucidated the agonist–quinine binding pocket of the bitter taste receptor T2R4.¹¹ While screening for compounds that are structurally similar to quinine, the phytohormone abscisic acid (ABA) was identified as a potential candidate. ABA is found in all plants and is known to mediate

responses to environmental stress and numerous plant developmental processes.¹² For example, the concentration of ABA can reach 30 $\mu\text{g/g}$ in ripe blueberries.¹³ As such, ABA is ingested by humans on a daily basis and has been proposed to mediate many beneficial health effects.¹⁴ Interestingly, it was recently proposed that ABA is also produced and released from monocytes, granulocytes, microglia, and insulin-secreting cells in humans.^{15–17} Endogenously produced ABA is proposed to act locally and in the case of pancreatic β -cells has been shown to enhance their ability to secrete insulin.¹⁸ ABA is also involved in various immune and inflammatory responses and has been administered orally in mouse models to treat diabetes, atherosclerosis, and inflammatory bowel disease.^{14,19–21} However, some contradictory reports do exist, related to the effect of ABA on Ca^{2+} responses in microglial cells.²² At the same time, very little is known about the actual molecular mechanism of action of ABA, and its receptor targets, in humans. To date, the lanthionine synthetase C-like 2

Received: August 13, 2014

Revised: April 3, 2015

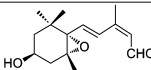
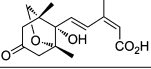
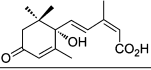
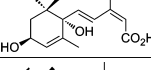
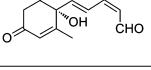
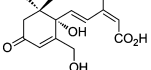
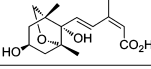
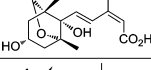
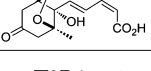
Published: April 6, 2015



(LANCL2) protein has been shown to bind ABA and modulate some ABA signaling in granulocytes and insulinoma cells.^{23,24} However, other human proteins, in particular HSP70 family members, have also been reported to bind to ABA.²⁵ Together, these findings suggest that a very complex signaling network is likely in play.

As T2Rs are distributed throughout the body, we hypothesized that ABA or its metabolites may have effects on T2R function by activating or blocking these receptors. To elucidate this, we docked a number of ABA metabolites to a recently validated molecular model of T2R4 (Table 1). Next,

Table 1. Predicted Binding Affinities of Absciscic Acid (ABA), Its Precursors, and Metabolites to T2R4^a

Ligand	Predicted binding affinity $-\log(K_d)$	Predicted K_d (μ M)	Structure
Xanthoxin	6.77	0.16	
Phaseic acid	6.42	0.37	
(+)-S-Absciscic acid	5.72	1.87	
1',4'-ABA diol	5.70	1.99	
Absciscic aldehyde	5.30	4.92	
7-OH-ABA	ND	ND	
DPA	ND	ND	
epiDPA	ND	ND	
neoPA	ND	ND	

^aThe compounds shown above were docked to T2R4 using the Surflex-Dock program of SYBYL-X 1.3. The binding affinities of receptor–ligand complexes from the Surflex-Dock scoring method were expressed as $-\log(K_d)$. ND indicates no binding to T2R4 detected by Surflex-Dock.

functional characterization involving calcium imaging and IP_3 assays was applied to the top three compounds. Results from this study suggest that ABA acts as an antagonist, and xanthoxin, which is an ABA precursor, acts as an agonist. Mutational analysis suggests that both the agonist quinine and antagonist ABA bind to the same orthosteric site in T2R4.

EXPERIMENTAL PROCEDURES

Materials. Mammalian cell culture medium DMEM-F12, streptomycin, penicillin, L-glutamate, trypsin-EDTA, lipofectamine-2000, and calcium sensitive dye Fluo-4NW were purchased from Life Technologies (Burlington, ON). (\pm) ABA and fetal bovine serum (FBS) were purchased from Sigma-Aldrich Canada Co. (Oakville, ON). All other chemicals used in the study were purchased either from Sigma-Aldrich or Fisher Scientific (Toronto, ON). The chimeric G protein,

G α 16/44, was a gift from T. Ueda (Nagoya City University, Nagoya, Japan).

Synthesis of Xanthoxin and Phaseic Acid. (–)-Xanthoxin was prepared by Y. Gai from (R)-4-hydroxy- β -cyclogeranol using a known procedure.²⁶ (–)-Phaseic acid (PA) was prepared from (+)-ABA by biotransformation using maize suspension-cultured cells.²⁷

Molecular Biology and Cell Culture. Codon-optimized FLAG-TAS2R4 was described previously.^{28,29} The mutants were synthesized commercially (Genscript USA Inc.). All the genes were cloned into pcDNA3.1 and transiently co-expressed in HEK293T cells with the chimeric G protein G α 16/44 using lipofectamine-2000, as described previously.^{11,29} Cells were propagated in DMEM-F12 medium, at 37 °C under 5% CO₂. Flow cytometry studies for elucidating cell surface expression of the receptors were conducted using the anti-FLAG antibody, exactly as described recently.¹¹

Intracellular Calcium Mobilization Assays. Functional characterization of the expressed receptors was pursued by calcium imaging using Fluo-4NW. Empty vector (pcDNA3.1) transfected cells were used as a control (mock transfected cells). Six to eight hours after transfection, cells were plated in 96-well clear bottom black walled plates at a density of 1×10^5 viable cells per well (viability determined by a TC10 Bio-Rad cell counter). After incubation for 12–16 h at 37 °C in a CO₂ incubator, the cell culture medium was removed, and the calcium sensitive dye Fluo-4NW was added. Cells were then incubated at 37 °C for 40 min followed by incubation for 40 min at room temperature. Fluo-4NW dye was prepared by adding 10 mL of calcium-free assay buffer to the lyophilized dye; 2.5 mM probenecid supplied with the Fluo-4NW assay kit was added to this solution to block the leakage of the dye from cytosol. The cells were treated with different concentrations of quinine, and the intracellular calcium released was measured in terms of relative fluorescence units (RFUs) using a Flexstation 3 plate reader. For the first 20 s, basal calcium levels were measured, the ligand(s) was added by the Flexstation 3 liquid handling system, and the calcium release was measured for the next 120 s. Absolute RFUs were determined by deducting the basal RFU from the peak RFU obtained after stimulating with the ligand (absolute RFUs = maximum – minimum). Δ RFUs were obtained by deducting the absolute RFUs of mock-transfected cells from the WT or mutant (Δ RFUs = WT or mutant absolute RFUs – mock-transfected absolute RFUs). The complete details of the protocol were described in our previous articles.^{11,29}

To elucidate the action of ABA and its metabolites on T2R4 and mutants, HEK293T cells expressing the receptors were initially treated with a single concentration of each compound of 0.5 mM. For determining the IC₅₀ value for ABA, the quinine concentration was kept constant at 1 mM (EC₅₀ value) and a concentration range of ABA from 0.5 to 0.007 mM was used. Calcium data were analyzed using PRISM software version 4.03 (GraphPad Software, La Jolla, CA).

IP₃ Assays. Known concentrations of IP₃ (20 pM to 20 μ M) were used to generate a standard graph by measuring the fluorescence according to the manufacturer's instructions (HitHunter IP₃ Fluorescence Polarization assay kit, DiscoveRx). Agonist-dependent and -independent IP₃ production by the cells expressing different receptor constructs or mock-transfected was measured using the standard graph. In each experiment, 1×10^5 viable cells were taken per well in black-walled plates. IP₃ produced was reported in terms of picomoles.

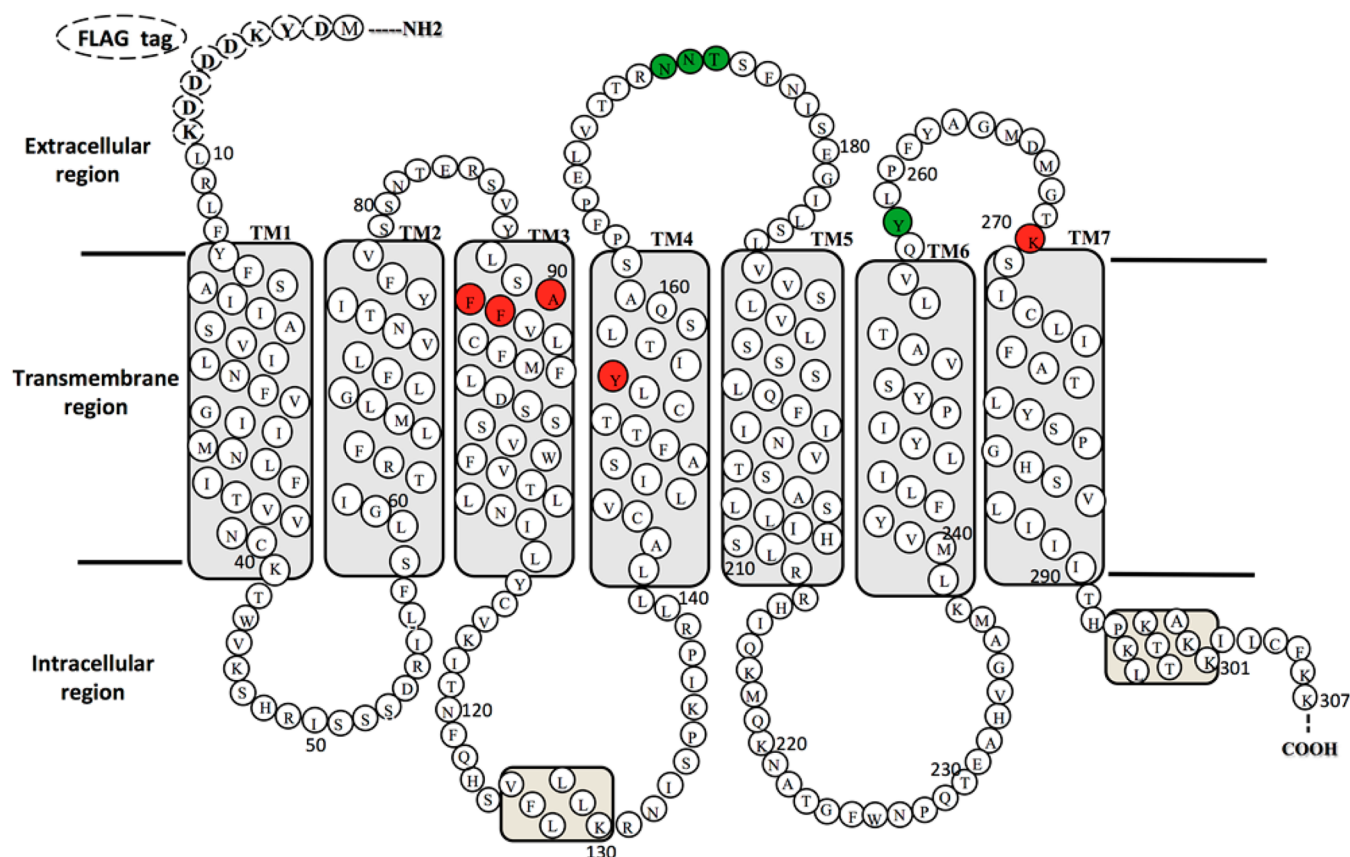


Figure 1. Schematic representation of the T2R4 amino acid sequence with an N-terminal FLAG tag. Similar to other T2Rs, T2R4 contains short N- and C-termini, seven transmembrane helices (TM1–7), three extracellular loops (ECL1–3), and three intracellular loops (ICL1–3). Residues involved in binding to agonist quinine are colored red and those involved in binding with abscisic acid (ABA) green.

Complete details of the assay were described in our previous publications.^{11,29}

Schild Regression Analysis. For Schild analysis, HEK293T cells stably expressing T2R4 and Ga16/44 chimera were used. To generate stable cells, HEK293T cells were cotransfected with T2R4 in pcDNA4/HisMaxB/Zeo and Ga16/44 chimera in pcDNA3.1/Hygro vectors and selected by resistance to both zeocin and hygromycin at 300 $\mu\text{g}/\text{mL}$ in the growth medium; 1×10^5 viable cells per well were plated in 96-well tissue culture-treated BD-falcon biolux microplates in DMEM-F12 medium containing 10% FBS for 24 h followed by a calcium assay. The cells were treated with T2R4 agonist quinine alone at different concentrations or in the presence of ABA (concentration kept constant). The experiments were repeated five times in triplicate, and the calcium readout was measured as relative fluorescence units (ΔRFU). The standard errors of the mean (SEM) of the dose–response data were fit to a sigmoid curve using Gaddum/Schild EC_{50} shift nonlinear regression in GraphPad Prism version 5.0. The calculation is based upon the equation for simple antagonism derived by Gaddum, where $[A]$ and $[B]$ represent molar concentrations of agonist and antagonist, respectively, with their equilibrium dissociation constants K_A and K_B , respectively, for the receptor. y represents the percentage of receptors occupied by an agonist.³⁰

$$[A]/K_A = (1 + [B]/K_B) \times y/100 - y$$

EC_{50} values from these fits were used in calculating a Schild analysis linear regression plot. The antagonist concentration

and dose ratio minus one ($\text{DR} - 1$) were plotted on the X-axis and Y-axis, respectively, on a log scale.

Molecular Modeling and Docking. Inactive T2R4 molecular models validated in our previous site-directed mutagenesis study were used. The T2R4 amino acid sequence without the FLAG tag was used for model building. The inactive T2R4 model was built using the rhodopsin crystal structure (Protein Data Bank entry 1U19) using the I-TASSER server. TMpred and HMMTOP servers were used to predict the transmembrane regions. The Mod Loop server was used to model the loop regions. Side chains of the amino acids were refined with SCWRL4. The receptor was prepared for ligand docking by adding hydrogen atoms followed by minimization using steepest descent and conjugate gradient algorithms.

ABA and its metabolite structures were obtained from pubchem or built using SYBYL-X 1.3 suite (CERTARA). These molecules were energy-minimized and docked with the T2R4 molecular model using Surflex-Dock of the SYBYL-X 1.3 suite. At least 10 poses were saved for each molecule. The binding affinities of the receptor–ligand complexes were obtained from Surflex-Dock score and expressed as $-\log(K_d)$.

Statistical Analysis. All the statistical analyses were performed using GraphPad Prism version 5.0. Significance among different columns in bar plots was analyzed using one-way analysis of variance followed by Tukey's multiple-comparison post hoc test ($p < 0.05$ was considered significant).

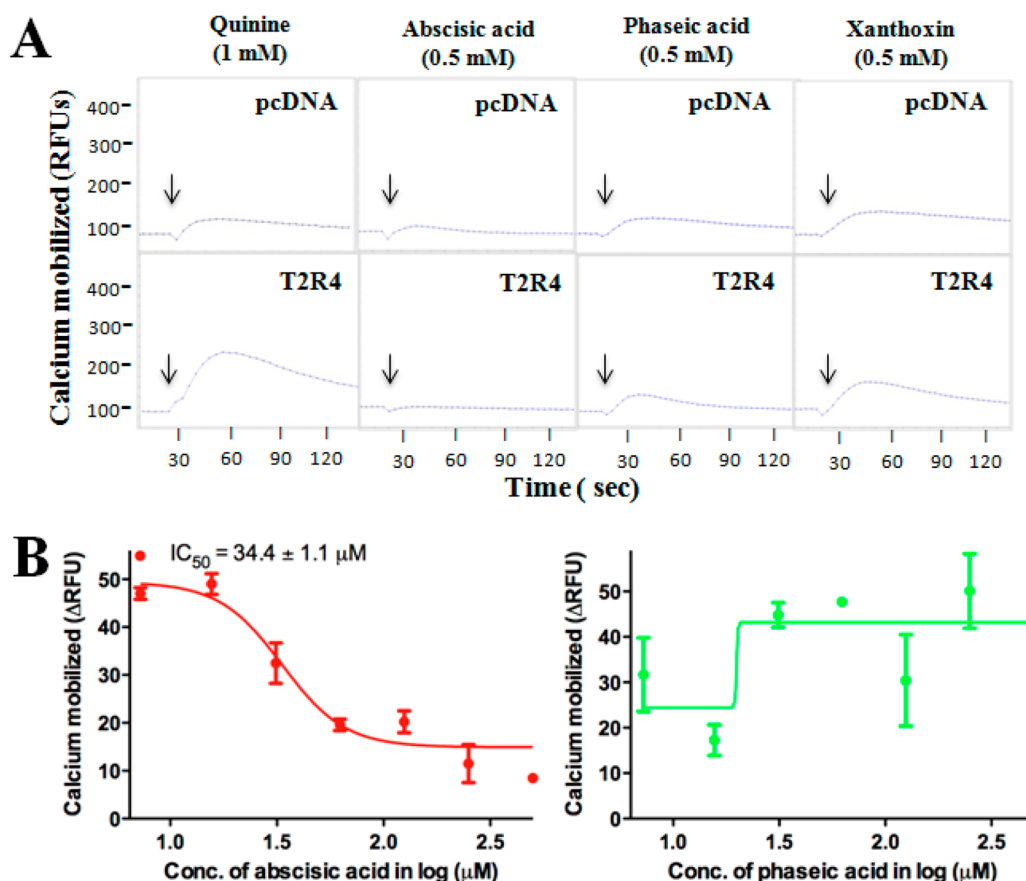


Figure 2. Calcium mobilization assays. (A) Representative calcium traces of pcDNA (mock-transfected) and T2R4 expressed in HEK293T cells and stimulated with quinine (1 mM) or 0.5 mM ABA, xanthoxin, or phaseic acid (PA). Arrows indicate the time point (20 s) at which the ligands were added. (B) Dose–response curves of T2R4 stimulated with increasing concentrations of ABA and PA in the presence of agonist quinine. HEK293T cells transiently expressing T2R4 were treated with different concentrations of the compounds in the presence of 1 mM quinine. T2R4 activity or calcium mobilization decreased with the increase in ABA concentration, and no change in calcium mobilization was observed in the case of PA. This indicates ABA inhibits quinine-mediated T2R4 activity with an IC_{50} of $34.4 \pm 1.1 \mu M$.

RESULTS

Prediction of Binding Affinities of ABA and Its Metabolites for T2R4. In our recent study, we identified T2R4 residues involved in binding to an agonist (quinine) and an antagonist (GABA) (Figure 1).¹¹ Both of these ligands were found to bind within the same orthosteric site in T2R4. Now, in this study, the quinine binding pocket in T2R4 was selected to dock ABA and its metabolites. Of the nine compounds screened, five of them were predicted to bind to T2R4 with binding affinities ranging from 0.16 to 4.92 μM (Table 1). The top three compounds, ABA, phaseic acid, and xanthoxin, that showed high predicted binding affinity were selected for further functional studies. Xanthoxin is a precursor of ABA, while phaseic acid is a catabolite formed by the oxidation of ABA.

Functional Effects of ABA, Xanthoxin, and Phaseic Acid on T2R4. To evaluate the functional effects of these compounds on T2R4, intracellular calcium was measured in HEK293T cells expressing T2R4, and in mock-transfected cells. Initially, a single concentration (0.5 mM) of ABA, xanthoxin, or phaseic acid was applied to both T2R4-expressing and mock-transfected cells. Because the EC_{50} value for quinine activation of T2R4 is known, it was used as an external agonist control, treating transfected cells with 1 mM quinine. While xanthoxin showed a measurable increase in calcium mobilization over mock-transfected cells, suggesting it acts as an agonist, ABA and

phaseic acid did not cause a significant increase in calcium mobilization (Figure 2A).

Showing no agonist activity, ABA and phaseic acid were subsequently tested for inhibition of agonist-stimulated T2R4. Competition assays were performed in the presence of the EC_{50} concentration of the agonist quinine (1 mM) and different concentrations (0.007–0.5 mM) of ABA and phaseic acid. Interestingly, ABA was able to decrease the calcium levels produced by quinine-activated T2R4 in a concentration-dependent manner (Figure 2B), whereas phaseic acid did not show any significant difference in the calcium levels (Figure 2B). ABA was able to block T2R4 activity with a half-maximal inhibitory concentration (IC_{50}) of $34.4 \pm 1.1 \mu M$.

Comparison of the calcium traces reveals xanthoxin to be a weak agonist compared to quinine (Figure 2A). Being a weak agonist would require larger quantities of this compound for pursuing studies to derive the EC_{50} value. Because of the limited quantities of xanthoxin synthesized, we were not able to obtain its EC_{50} value. To overcome this limitation, we used the more sensitive and reliable IP_3 assay, which requires relatively less compound. We treated T2R4-expressing cells with buffer (to measure basal activity), or 1, 2, and 3 mM xanthoxin, and the IP_3 produced was measured in picomoles (Figure 3A). Xanthoxin (1 mM) was able to activate T2R4, but not significantly when compared to basal levels. In contrast, 2 and 3 mM xanthoxin-treated T2R4 cells showed a statistically

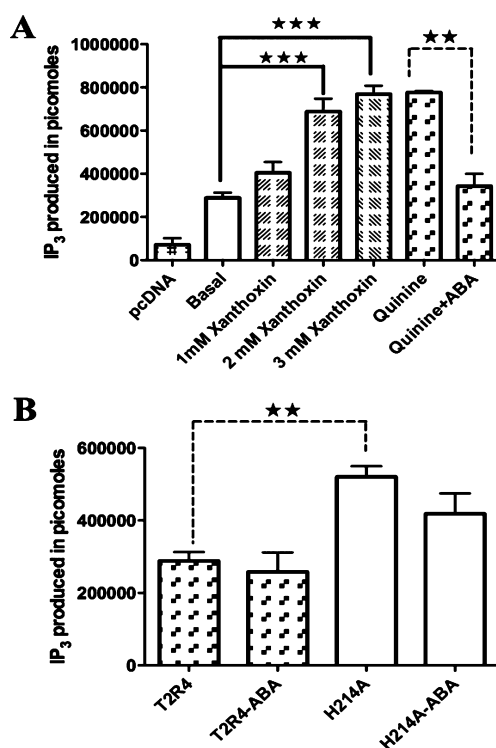


Figure 3. Pharmacological characterization of ABA and xanthoxin. (A) Inositol 1,4,5-triphosphate (IP₃) production by T2R4-expressing HEK293T cells when treated with buffer (basal), different concentrations of xanthoxin (1–3 mM), quinine (1 mM), and quinine (1 mM) with ABA (35 μ M). pcDNA-transfected cells (mock transfection) were used as a control; 2 and 3 mM xanthoxin showed a significant increase in IP₃ production, comparable to that for T2R4 stimulated with 1 mM quinine. When T2R4-expressing cells were treated with quinine (1 mM) and ABA (35 μ M), the amount of IP₃ produced was reduced significantly. (B) Effect of ABA treatment on basal intracellular IP₃ production. T2R4 and H214A CAM-expressing HEK293T cells were treated with 35 μ M ABA, and the IP₃ produced was measured as described in Experimental Procedures. H214A basal activity was not decreased significantly in the presence of ABA. This confirms that ABA is an antagonist and not an inverse agonist.

significant increase in IP₃ production compared to the basal level and that seen with 1 mM xanthoxin (Figure 3A). To confirm the antagonist activity of ABA, we stimulated T2R4-expressing cells with 1 mM quinine (EC₅₀ value), and 1 mM quinine and 35 μ M ABA (IC₅₀ value). As expected, levels of IP₃ produced in the presence of ABA decreased significantly, compared to that with quinine alone (Figure 3A).

Pharmacological Characterization of ABA. GPCRs are known to show some activity in the absence of agonist, and this phenomenon is often termed basal or constitutive activity. Some of the T2R mutants also show basal activity higher than those of native receptors, and these mutants are termed constitutively active mutants (CAMs).³¹ CAMs can be used as pharmacological tools to classify the blockers as antagonists or inverse agonists. An antagonist will block the CAM but does not reduce basal activity further than the wild-type receptor. In contrast, inverse agonists will reduce the basal activity of the CAM, significantly below wild-type levels. H214A is a well-characterized CAM in T2R4 and was successfully used to classify bitter blockers in our previous study.¹¹ To characterize the pharmacological activity of ABA, we stimulated T2R4 and H214A CAM with buffer alone and with 35 μ M ABA (IC₅₀

value) dissolved in buffer. In both T2R4 and H214A, ABA did not decrease the basal activity, which confirms that ABA is an antagonist but not an inverse agonist of T2R4 (Figure 3B).

To determine the nature of ABA antagonism in T2R4 against quinine, Schild regression analysis was performed. When the cells were treated with an increasing concentration of quinine (0.07–5 mM), this increased the level of intracellular calcium mobilization. At constant concentrations of ABA (3, 30, 100, and 300 μ M), the concentration response curves were shifted to the right without affecting the maximal response (Figure 4). The effects of ABA are surmountable at high quinine concentrations. However, this alone would not conclude the nature of ABA antagonism. When these data were analyzed, the Schild regression generated a slope of 0.46 ± 0.02 with a 95% confidence interval (CI) (0.33–0.59). The determined pA_2 value is 1.99 based on the intercept on the abscissa (Figure 4, inset).

Ligand Binding Pocket of ABA. To elucidate the T2R4 amino acids involved in binding to ABA, molecular model-guided mutagenesis was pursued. Interestingly, according to the model, the binding pocket of ABA is predicted to be very similar to the quinine binding pocket, with some minor differences in the hydrogen bonding pattern (Figure 5). ABA formed H-bonds with three ECL2 residues, Asn172, Asn173, and Thr174, and Tyr258 of ECL3. Lys270 of ECL3 was also present in the 4 Å region of the ABA binding pocket; however, no H-bond was observed, and the K270A mutation showed hyperactivity.¹¹ The Asn172 and Tyr258 side chains were involved in the H-bonding, whereas the backbone of Asn173 and Thr174 mediated the interactions here. The role of most of these amino acids in ABA binding could not be elucidated as these were found to be essential for quinine binding.¹¹ However, we were able to characterize the contributions of Thr174 and Lys270 to signaling in response to ABA treatment. In our previous study, we showed that T174A shows defective signaling, while the homologous T174S substitution was able to signal in response to quinine treatment. Therefore, in this study, three mutations, T174S, K270A, and K270R, were studied with respect to calcium mobilization after ABA treatment. These mutants and WT T2R4 were expressed in HEK293T cells, and competition assays were pursued with different concentrations of quinine in the presence of 35 μ M ABA (IC₅₀ value). ABA was able to reduce the quinine-dependent activity of K270A and K270R, but no significant difference was found compared to that of T2R4 treated with quinine and ABA (Figure 6). This suggests that Lys270 is not important for ABA-mediated signaling. Interestingly, mutant T174S completely lost the ability to signal upon being treated with quinine in the presence of ABA (Figure 6A). This suggests that Thr174 might be involved in ABA binding and signaling.

ABA Activity on Other Known T2R4 Agonists. To test the ABA antagonism on other T2R4 agonists, we screened four additional compounds that were reported to activate T2R4, namely, colchicine, denatonium benzoate, PROP, and yohimbine.⁸ We observed that of these four compounds, only yohimbine activated T2R4 and that too not in a concentration-dependent manner. Under our assay conditions, colchicine, PROP, and denatonium benzoate were unable to show any significant activation of T2R4 (Figure S1 of the Supporting Information). To test ABA antagonism on yohimbine, we pursued competition assays using a range of yohimbine concentrations and a fixed concentration of ABA (35 μ M) based on its IC₅₀ value for quinine. Our results suggest that

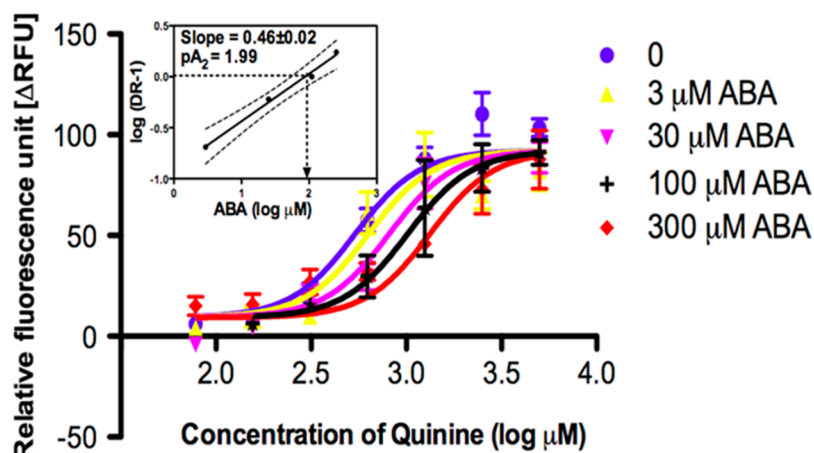


Figure 4. Schild regression analysis of ABA antagonism to quinine in T2R4. The concentration dependence of the increase in the level of intracellular calcium mobilization in response to quinine at different concentrations (0.07–5 mM) was compared in the absence (blue) and presence of 3 μ M (yellow), 30 μ M (magenta), 100 μ M (black), and 300 μ M (red) ABA. The concentration–response curves were shifted to the right with increasing concentrations of ABA. In the inset, the dose ratio minus one ($DR - 1$) was obtained from the EC_{50} value of each curve and plotted vs antagonist concentration on a log scale to calculate Schild linear regression. The Schild plot generated a slope of 0.46 ± 0.02 with a 95% CI (0.33–0.59) indicated with dashed lines. The pA_2 value was determined as 1.99 indicated as the intercept with an abscissa as a dotted line. Data were collected from at least five independent experiments with each data point in triplicate. EC_{50} values were calculated and regression analyses conducted using Graphpad Prism 5.0.

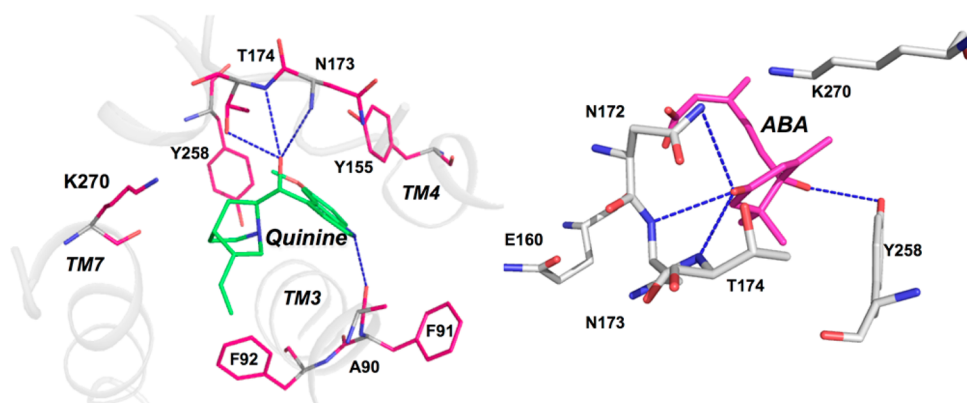


Figure 5. Molecular model of T2R4 bound to quinine and ABA. The compounds were docked to a T2R4 three-dimensional model using the Surflex-Dock program of the SYBYL-X 1.3 suite, and the docked complexes were analyzed using PyMol. TM1–7 are colored gray; quinine is colored green, and the amino acids within 4 Å of quinine are colored pink. In the ABA-docked T2R4 model, ABA is colored pink and the amino acids within 4 Å are colored gray. The H-bonds are represented as blue dotted lines.

ABA does not inhibit yohimbine-induced T2R4 activity (Figure S1 of the Supporting Information). However, given the atypical response of yohimbine on T2R4, not much inference could be drawn.

DISCUSSION

GPCRs make up one of the largest gene families in humans and play crucial roles in cell–cell communication. Because of their crucial roles in various cellular and physiological processes, they continue to be targeted for development of numerous drugs. T2Rs are one of the least characterized classes in the GPCR superfamily. Recent studies showed expression of T2Rs in various cell types, and understanding their role in different physiological processes is at the early stage.^{32,33} Functional expression of T2Rs in heterologous systems allowed deorphanization of most of the receptors. More than 100 natural and synthetic bitter compounds are known to activate these T2Rs. However, information about bitter blockers is very limited. In this study, we characterized the biochemical and pharmacological

profile of ABA and some of its metabolites on one of the well-characterized bitter taste receptors, T2R4.

On the basis of previously published information about agonist and antagonist binding in T2Rs, we pursued virtual ligand screening of ABA and its eight metabolites. Among these, only five compounds were predicted to bind, and we chose the top three predicted candidates, ABA, phaseic acid, and xanthoxin, for functional characterization. Competition assays with quinine showed that ABA is a T2R4 blocker with an IC_{50} value of $34.4 \pm 1.1 \mu$ M. IP_3 assays confirmed this finding. While we were not able to determine the EC_{50} value for xanthoxin, as the availability of compound was limiting, the initial screening by calcium imaging suggested xanthoxin to be a weak agonist (Figure 2A). This was also confirmed by IP_3 assays, where no significant difference in IP_3 production was observed between 2 and 3 mM xanthoxin, revealing its EC_{50} value to be in the range of 1–2 mM (Figure 3A). Pharmacological characterization of ABA using a well-studied CAM, H214A, confirmed that ABA is an antagonist and not an

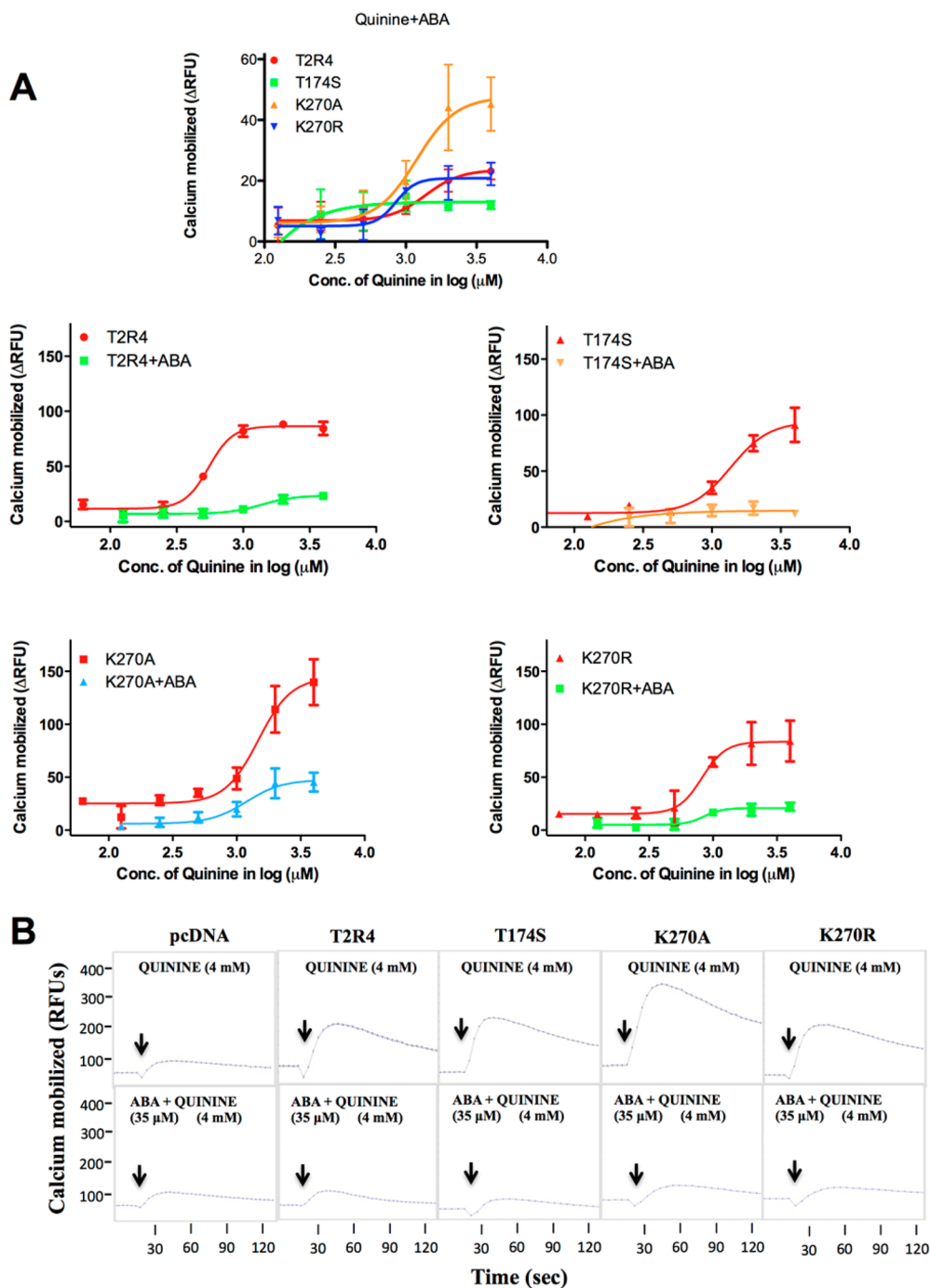


Figure 6. Functional characterization of T2R4 residues predicted to be important for ABA binding. (A) Cells expressing T2R4, T174S, K270A, and K270R were stimulated with different concentrations of quinine (0.06–4 mM) in the presence and absence of IC_{50} concentrations of ABA (35 μ M). Changes in intracellular calcium mobilized were measured (Δ RFUs). All the experiments were repeated at least three times in triplicate. In all cases, ABA significantly reduced the activity of the receptors. (B) Raw calcium traces of pcDNA, T2R4, T174S, K270A, and K270R in the presence of 4 mM quinine and/or 35 μ M ABA. Arrows represent the time point (20 s) of addition of quinine or quinine with ABA.

inverse agonist (Figure 3B). It is interesting to note that similar results were observed in the case of gentiobiose and isomaltose. Gentiobiose is bitter and isomaltose sweet, and they are anomers. T2R16 can be activated by gentiobiose but not by isomaltose.³⁴

From a structural perspective, ABA and xanthoxin have similar overall structures but differ in the oxidation state of the side chain (acid vs aldehyde) and with some ring modifications, including for xanthoxin an epoxide at the 1' and 2' ring carbons in place of a hydroxyl group off the chiral center on ABA, and a

hydroxyl group in place of the ketone at the 4' ring carbon. While any contribution of modification of the compound side chain is unclear, modeling suggests the impact of the ring modifications could be critical. In the ABA model, the ketone oxygen at the 4' ring carbon makes three H-bonds with residues 172–174, a position that is stabilized by the hydroxyl group at the chiral center extending to make a H-bond with the side chain of residue Tyr258. These four H-bonds stabilize ABA in a position where it sterically clashes with the side chain hydroxyl of T174 (Figure 5). The fact that ABA is ineffective

against the T174S mutant supports the importance of this clash between ABA and the threonine side chain, in mediating the antagonistic effect of ABA. However, this model remains to be validated, and what the exact role of the Thr174 side chain is in mediating antagonism remains to be determined.

From a structure–function perspective, information about agonist and antagonist binding is useful for improving the selectivity and discovering more potent antagonists. For example, in our previous study, we identified key T2R4 residues crucial for agonist (quinine), antagonist (GABA), and inverse agonist (BCML) binding. The binding pocket of all three compounds overlapped, but subtle differences in the interactions were predicted.¹¹ This is similar to the situation here comparing xanthoxin to ABA. Interestingly, for quinine, GABA, and BCML, ECL2 residues contributed to ligand binding. Therefore, this region appears to be essential for agonist and antagonist binding generally. Other contributions of residues from the TMs and ECLs are specific for each compound dictating their activity. For example, Lys270 is important for GABA and quinine binding, while Ala90 is important for BCML and quinine binding.¹¹ Interestingly, neither of these residues is important for ABA binding, likely related to the smaller size of the ABA molecule compared to quinine. The observation that Thr174 might be involved in ABA-mediated signaling emphasizes that the mechanism of ABA antagonism is unique compared to that of GABA. Overall, we conclude that specific residues in the orthosteric site of T2R4 play important roles in mediating the observed ligand specificities and activities.

In our Schild analysis, although the maximal response of quinine was not affected by increasing concentrations of ABA, we observed a rightward shift in the dose–response curves for quinine, and the Schild plot generated a slope of 0.46 ± 0.02 at a 95% CI of 0.33–0.59 with a pA_2 value 1.99 (Figure 4). A slope significantly less than unity indicates a number of possibilities such as (i) noncompetitive antagonism, (ii) multimolecular interactions among drugs and receptors, and (iii) nonequilibrium conditions in the experimental procedures. When the reduction of the slope is antagonist-related, this would cause a diminished potency of antagonist. With the increasing concentrations of antagonist being greater than the K_B for its antagonism, the Schild equation would not predict a simple competitive antagonism. A possibility can be an agonist-related reduction in the slope. At high concentrations (in the millimolar range), agonists might produce nonspecific responses such as those mediated by other proteins or receptors, which cannot be blocked by the antagonist.³⁰ In addition to T2Rs, at higher concentrations, quinine can also activate other cellular effectors. Because we performed a simultaneous treatment with quinine and ABA on the HEK293T-T2R4-Ga16/44 stable cells, a multimolecular interaction could be another reason for the reduction in the slope obtained in Schild regression analysis. Similar conditions were reported in a previous study in which agouti-signaling protein (ASIP) was determined to be a surmountable antagonist at human melanocortin receptors exhibiting complex mechanisms with slopes significantly less than unity.³⁵ When the slope is equal to unity, the pA_2 value gives the antagonist concentration to produce a dose ratio equal to 2 based on the intercept with the abscissa. Considering the observations discussed above, with slope of less than unity we cannot determine the K_B value of ABA or conclude the interaction is simple competitive inhibition.³⁶

Important criteria for a bitter blocker include that it preferably be of natural origin and should be available in sufficient quantities;¹⁰ ABA fulfills both criteria. In addition to being readily available in the human diet through consumption of plants, ABA also appears to be produced by human cells. These include leukocytes, pancreatic cells, and mesenchymal cells. It is suggested ABA acts as a signaling molecule in various diseased conditions.^{14,18} ABA production was also observed in the pig brain.³⁷ Recent studies showed the expression of T2R4 in human leukocytes, airways, trachea, colon, gut, and heart, and in rat brain.^{3,5,31,38} It is possible that ABA might be playing a key role in regulating the function of T2R4 in some of these tissues.

In summary, this study has led to the identification of a new receptor target for ABA in humans, and characterization of ABA as a T2R blocker. Interestingly, we found that the ABA precursor, xanthoxin, acts as a T2R4 agonist while pharmacological characterization led to the identification of ABA as an antagonist for T2R4. Molecular model-guided mutational studies showed that Thr174 in T2R4 plays an important and unique role in binding and signaling through ABA. The antagonist activity of ABA on the 24 remaining T2Rs remains to be tested as does its mechanism of antagonism. Given that ABA is a natural compound and abundantly present in plants, it has significant nutraceutical potential.

■ ASSOCIATED CONTENT

● Supporting Information

Representative calcium traces of T2R4 transfected in HEK293T cells and induced with different concentrations of bitter compounds and the response of T2R4 to yohimbine in the absence and presence of ABA (Figure S1). This material is available free of charge via the Internet at <http://pubs.acs.org>.

■ AUTHOR INFORMATION

Corresponding Author

*D319, Department of Oral Biology, 780 Bannatyne Ave., University of Manitoba, Winnipeg, MB R3E 0W4, Canada. E-mail: prashen.chelikani@umanitoba.ca. Telephone: (204) 789-3539. Fax: (204) 789-3913.

Funding

This work was supported by a discovery grant (RGPIN-2014-04099) from the Natural Sciences and Engineering Research Council of Canada and a Manitoba Medical Service Foundation Allen Rouse Career Award to P.C. S.P.P. and A.J. were supported by graduate studentships from Research Manitoba and the University of Manitoba.

Notes

The authors declare no competing financial interest.

■ ABBREVIATIONS

GPCRs, G protein-coupled receptors; T2Rs, bitter taste receptors; ABA, abscisic acid; PA, phaseic acid; HEK293T, human embryonic kidney cells expressing the T-antigen.

■ REFERENCES

- (1) Chandrashekar, J., Mueller, K. L., Hoon, M. A., Adler, E., Feng, L., Guo, W., Zuker, C. S., and Ryba, N. J. (2000) T2Rs function as bitter taste receptors. *Cell* 100, 703–711.
- (2) Adler, E., Hoon, M. A., Mueller, K. L., Chandrashekar, J., Ryba, N. J., and Zuker, C. S. (2000) A novel family of mammalian taste receptors. *Cell* 100, 693–702.

- (3) Singh, N., Vrontakis, M., Parkinson, F., and Chelikani, P. (2011) Functional bitter taste receptors are expressed in brain cells. *Biochem. Biophys. Res. Commun.* 406, 146–151.
- (4) Deshpande, D. A., Wang, W. C., McIlmoyle, E. L., Robinett, K. S., Schillinger, R. M., An, S. S., Sham, J. S., and Liggett, S. B. (2010) Bitter taste receptors on airway smooth muscle bronchodilate by localized calcium signaling and reverse obstruction. *Nat. Med.* 16, 1299–1304.
- (5) Foster, S. R., Porrello, E. R., Purdue, B., Chan, H. W., Voigt, A., Frenzel, S., Hannan, R. D., Moritz, K. M., Simmons, D. G., Molenaar, P., Roura, E., Boehm, U., Meyerhof, W., and Thomas, W. G. (2013) Expression, regulation and putative nutrient-sensing function of taste GPCRs in the heart. *PLoS One* 8, e64579.
- (6) Foster, S. R., Roura, E., and Thomas, W. G. (2014) Extrasensory perception: Odorant and taste receptors beyond the nose and mouth. *Pharmacol. Ther.* 142, 41–61.
- (7) Wu, S. V., Rozengurt, N., Yang, M., Young, S. H., Sinnett-Smith, J., and Rozengurt, E. (2002) Expression of bitter taste receptors of the T2R family in the gastrointestinal tract and enteroendocrine STC-1 cells. *Proc. Natl. Acad. Sci. U.S.A.* 99, 2392–2397.
- (8) Meyerhof, W., Batram, C., Kuhn, C., Brockhoff, A., Chudoba, E., Bufo, B., Appendino, G., and Behrens, M. (2010) The molecular receptive ranges of human TAS2R bitter taste receptors. *Chem. Senses* 35, 157–170.
- (9) Brockhoff, A., Behrens, M., Roudnitzky, N., Appendino, G., Avonto, C., and Meyerhof, W. (2011) Receptor agonism and antagonism of dietary bitter compounds. *J. Neurosci.* 31, 14775–14782.
- (10) Roland, W. S., Gouka, R. J., Gruppen, H., Driesse, M., van Buren, L., Smit, G., and Vincken, J. P. (2014) 6-Methoxyflavanones as bitter taste receptor blockers for hTAS2R39. *PLoS One* 9, e94451.
- (11) Pydi, S. P., Sobotkiewicz, T., Billakanti, R., Bhullar, R. P., Loewen, M. C., and Chelikani, P. (2014) Amino acid derivatives as bitter taste receptor (T2R) blockers. *J. Biol. Chem.* 289, 25054–25066.
- (12) Wasilewska, A., Vlad, F., Sirichandra, C., Redko, Y., Jammes, F., Valon, C., Frei dit Frey, N., and Leung, J. (2008) An update on abscisic acid signaling in plants and more. *Mol. Plant* 1, 198–217.
- (13) Zifkin, M., Jin, A., Ozga, J. A., Zaharia, L. I., Scherthner, J. P., Gesell, A., Abrams, S. R., Kennedy, J. A., and Constabel, C. P. (2012) Gene expression and metabolite profiling of developing highbush blueberry fruit indicates transcriptional regulation of flavonoid metabolism and activation of abscisic acid metabolism. *Plant Physiol.* 158, 200–224.
- (14) Bassaganya-Riera, J., Skoneczka, J., Kingston, D. G., Krishnan, A., Misyak, S. A., Guri, A. J., Pereira, A., Carter, A. B., Minorsky, P., Tumarkin, R., and Hontecillas, R. (2010) Mechanisms of action and medicinal applications of abscisic Acid. *Curr. Med. Chem.* 17, 467–478.
- (15) Bruzzzone, S., Ameri, P., Briatore, L., Mannino, E., Basile, G., Andraghetti, G., Grozio, A., Magnone, M., Guida, L., Scarfi, S., Salis, A., Damonte, G., Sturla, L., Nencioni, A., Fenoglio, D., Fiory, F., Miele, C., Beguinot, F., Ruvoletto, V., Bormioli, M., Colombo, G., Maggi, D., Murialdo, G., Cordera, R., De Flora, A., and Zocchi, E. (2012) The plant hormone abscisic acid increases in human plasma after hyperglycemia and stimulates glucose consumption by adipocytes and myoblasts. *FASEB J.* 26, 1251–1260.
- (16) Bruzzzone, S., Moreschi, I., Usai, C., Guida, L., Damonte, G., Salis, A., Scarfi, S., Millo, E., De Flora, A., and Zocchi, E. (2007) Abscisic acid is an endogenous cytokine in human granulocytes with cyclic ADP-ribose as second messenger. *Proc. Natl. Acad. Sci. U.S.A.* 104, 5759–5764.
- (17) Magnone, M., Bruzzzone, S., Guida, L., Damonte, G., Millo, E., Scarfi, S., Usai, C., Sturla, L., Palombo, D., De Flora, A., and Zocchi, E. (2009) Abscisic acid released by human monocytes activates monocytes and vascular smooth muscle cell responses involved in atherogenesis. *J. Biol. Chem.* 284, 17808–17818.
- (18) Bruzzzone, S., Bodrato, N., Usai, C., Guida, L., Moreschi, I., Nano, R., Antonioli, B., Fruscione, F., Magnone, M., Scarfi, S., De Flora, A., and Zocchi, E. (2008) Abscisic acid is an endogenous stimulator of insulin release from human pancreatic islets with cyclic ADP ribose as second messenger. *J. Biol. Chem.* 283, 32188–32197.
- (19) Guri, A. J., Hontecillas, R., and Bassaganya-Riera, J. (2010) Abscisic acid synergizes with rosiglitazone to improve glucose tolerance and down-modulate macrophage accumulation in adipose tissue: Possible action of the cAMP/PKA/PPAR gamma axis. *Clin. Nutr.* 29, 646–653.
- (20) Bassaganya-Riera, J., Guri, A. J., Lu, P., Climent, M., Carbo, A., Sobral, B. W., Horne, W. T., Lewis, S. N., Bevan, D. R., and Hontecillas, R. (2011) Abscisic acid regulates inflammation via ligand-binding domain-independent activation of peroxisome proliferator-activated receptor gamma. *J. Biol. Chem.* 286, 2504–2516.
- (21) Guri, A. J., Misyak, S. A., Hontecillas, R., Hastly, A., Liu, D., Si, H., and Bassaganya-Riera, J. (2010) Abscisic acid ameliorates atherosclerosis by suppressing macrophage and CD4+ T cell recruitment into the aortic wall. *J. Nutr. Biochem.* 21, 1178–1185.
- (22) Jiang, S. X., Benson, C. L., Zaharia, L. I., Abrams, S. R., and Hou, S. T. (2010) Abscisic acid does not evoke calcium influx in murine primary microglia and immortalised murine microglial BV-2 and N9 cells. *Biochem. Biophys. Res. Commun.* 401, 435–439.
- (23) Sturla, L., Fresia, C., Guida, L., Bruzzzone, S., Scarfi, S., Usai, C., Fruscione, F., Magnone, M., Millo, E., Basile, G., Grozio, A., Jacchetti, E., Allegretti, M., De Flora, A., and Zocchi, E. (2009) LANC2 is necessary for abscisic acid binding and signaling in human granulocytes and in rat insulinoma cells. *J. Biol. Chem.* 284, 28045–28057.
- (24) Sturla, L., Fresia, C., Guida, L., Grozio, A., Vigliarolo, T., Mannino, E., Millo, E., Bagnasco, L., Bruzzzone, S., De Flora, A., and Zocchi, E. (2011) Binding of abscisic acid to human LANC2. *Biochem. Biophys. Res. Commun.* 415, 390–395.
- (25) Kharenko, O. A., Polichuk, D., Nelson, K. M., Abrams, S. R., and Loewen, M. C. (2013) Identification and characterization of interactions between abscisic acid and human heat shock protein 70 family members. *J. Biochem.* 154, 383–391.
- (26) Kuba, M., Furuichi, N., and Katsumura, S. (2002) Stereocontrolled Synthesis of Carotenoid Oxidative Metabolites, (–)-Lololide, (–)-Xanthoxin, and their Stereoisomers. *Chem. Lett.* 31, 1248–1249.
- (27) Balsevich, J. J., Cutler, A. J., Lamb, N., Friesen, L. J., Kurz, E. U., Perras, M. R., and Abrams, S. R. (1994) Response of Cultured Maize Cells to (+)-Abscisic Acid, (–)-Abscisic Acid, and Their Metabolites. *Plant Physiol.* 106, 135–142.
- (28) Pydi, S. P., Bhullar, R. P., and Chelikani, P. (2012) Constitutively active mutant gives novel insights into the mechanism of bitter taste receptor activation. *J. Neurochem.* 122, 537–544.
- (29) Pydi, S. P., Singh, N., Upadhyaya, J., Bhullar, R. P., and Chelikani, P. (2014) The third intracellular loop plays a critical role in bitter taste receptor activation. *Biochim. Biophys. Acta* 1838, 231–236.
- (30) Kenakin, T. P. (1982) The Schild regression in the process of receptor classification. *Can. J. Physiol. Pharmacol.* 60, 249–265.
- (31) Pydi, S. P., Bhullar, R. P., and Chelikani, P. (2014) Constitutive activity of bitter taste receptors. *Adv. Pharmacol.* 70, 11–20.
- (32) Pydi, S. P., Upadhyaya, J., Singh, N., Pal Bhullar, R., and Chelikani, P. (2012) Recent advances in structure and function studies on human bitter taste receptors. *Curr. Protein Pept. Sci.* 13, 501–508.
- (33) Clark, A. A., Liggett, S. B., and Munger, S. D. (2012) Extraoral bitter taste receptors as mediators of off-target drug effects. *FASEB J.* 26, 4827–4831.
- (34) Sakurai, T., Misaka, T., Ueno, Y., Ishiguro, M., Matsuo, S., Ishimaru, Y., Asakura, T., and Abe, K. (2010) The human bitter taste receptor, hTAS2R16, discriminates slight differences in the configuration of disaccharides. *Biochem. Biophys. Res. Commun.* 402, 595–601.
- (35) Yang, Y. K., Ollmann, M. M., Wilson, B. D., Dickinson, C., Yamada, T., Barsh, G. S., and Gantz, I. (1997) Effects of recombinant agouti-signaling protein on melanocortin action. *Mol. Endocrinol.* 11, 274–280.
- (36) Wyllie, D. J., and Chen, P. E. (2007) Taking the time to study competitive antagonism. *Br. J. Pharmacol.* 150, 541–551.

- (37) Le Page-Degivry, M. T., Bidard, J. N., Rouvier, E., Bulard, C., and Lazdunski, M. (1986) Presence of abscisic acid, a phytohormone, in the mammalian brain. *Proc. Natl. Acad. Sci. U.S.A.* 83, 1155–1158.
- (38) Behrens, M., and Meyerhof, W. (2010) Oral and extraoral bitter taste receptors. *Results Probl. Cell Differ.* 52, 87–99.